Journal of Hazardous Materials 182 (2010) 877–885

Contents lists available at ScienceDirect

Journal of Hazardous Materials

journal homepage: www.elsevier.com/locate/jhazmat

Binding of bisphenol A and acrylamide to BSA and DNA: Insights into the comparative interactions of harmful chemicals with functional biomacromolecules

Ya-Lei Zhang [a], Xian Zhang [a], Xun-Chang Fei [a], Shi-Long Wang [b], Hong-Wen Gao [a,*]

[a] State Key Laboratory of Pollution Control and Resource Reuse, College of Environmental Science and Engineering, Tongji University, Shanghai 200092, China
[b] School of Life Science and Technology, Tongji University, Shanghai 200092, China

ARTICLE INFO

Article history:
Received 27 April 2010
Received in revised form 21 June 2010
Accepted 30 June 2010
Available online 8 July 2010

Keywords:
Bovine serum albumin
Deoxyribonucleic acid
Intermolecular interaction
Bisphenol A
Acrylamide

ABSTRACT

The interactions between bisphenol A (BPA)/acrylamide (AA) and bovine serum albumin (BSA)/deoxyribonucleic acid (DNA) was investigated by the equilibrium dialysis, fluorophotometry, isothermal titration calorimetry (ITC) and circular dichroism (CD). The bindings of BPA and AA to BSA and DNA responded to the partition law and Langmuir isothermal model, respectively. The saturation mole number of AA was calculated to be 24 per mol BSA and 0.26 per mol DNA-P. All the reactions were spontaneous driven by entropy change. BPA stacked into the aromatic hydrocarbon groups of BSA and between adjacent basepairs of DNA via the hydrophobic effect. The interactions of AA with BSA and DNA induced the formation of hydrogen bond and caused changes of their secondary structures. At normal physiological condition, 0.100 mmol/l BPA reduced the binding of vitamin B_2 to BSA by more than 70%, and 2.8 mmol/l AA by almost one half. This work provides an insight into non-covalent intermolecular interaction between organic contaminant and biomolecule, helping to elucidate the toxic mechanism of harmful chemicals.

1. Introduction

Serum albumin is the major transport protein in circulation system. It is the well-known model protein and is called a multifunctional plasma carrier protein for its ability to bind a wide variety of ligands. These include inorganic cations, organic anions, amino acids, vitamins and, perhaps most important, physiologically available insoluble endogenous compounds, e.g., fatty acids, bilirubin, and bile acids [1–6]. In fact, not only endogenous ligands but also exogenous compounds bind to HSA, e.g., commonly used drugs such as warfarin, camptothecins and inorganic polymers such as polyoxometalates [7–9]. The binding mechanism has been investigated, e.g., arazine, ochratoxin, methyl parathion, and arsenic [10–13]. Concerning to DNA, whose conformation and sequence preference is critical to replication, transcription and DNA chromatin compaction [14], it is reported that DNA is subject to the effect of organic chemicals, too, whether it is endogenous ligands or exogenous compounds. As the target of many drugs and also most likely of a large number of environmental pollutants [15–18], DNA has been extensively studied on the binding mechanism, e.g., minor groove binding, major groove binding, and (bis)intercalation. For example, Distamycin A can bind in the minor groove of duplex DNA primarily at AT-rich sequences as a monomer or as a side-by-side antiparallel dimer [19].

In fact, the involvement of any substances is likely to affect the activity of biomolecules [20,21]. Thousands of natural and synthetic organic chemicals are causing environmental pollution. Bisphenol A (BPA) and acrylamide (AA) extensively used in industry and distributed in the environment [22–24] have caused great concerns in recent years. Extensive investigations indicated that both of them have adverse effects on wildlife and human health [25–37]. BPA is listed as one of the most widely spread endocrine-disrupting chemicals and AA found in the carbohydrate-rich foods classified as a probable human carcinogen [38–41]. Considering different chemical structures and consequently different solubility in water, it's necessary to investigate the structure-effect of the toxicity mechanism of BPA and AA. Elucidation of the intermolecular interaction such as protein–protein and DNA–ligand binding, enzyme catalysis, and inhibition is crucial to understanding of cellular processes [42–45] using X-ray crystallography, NMR and surface plasmon resonance biosensors [46–49]. In this work, the equilibrium dialysis, fluorophotometry, isothermal titration calorimeter (ITC) and CD were used to characterize the bindings of BPA and AA to BSA and

* Corresponding author. Tel.: +86 21 65988598; fax: +86 21 65988598.
E-mail address: hwgao@tongji.edu.cn (H.-W. Gao).

0304-3894/$ – see front matter © 2010 Elsevier B.V. All rights reserved.
doi:10.1016/j.jhazmat.2010.06.131

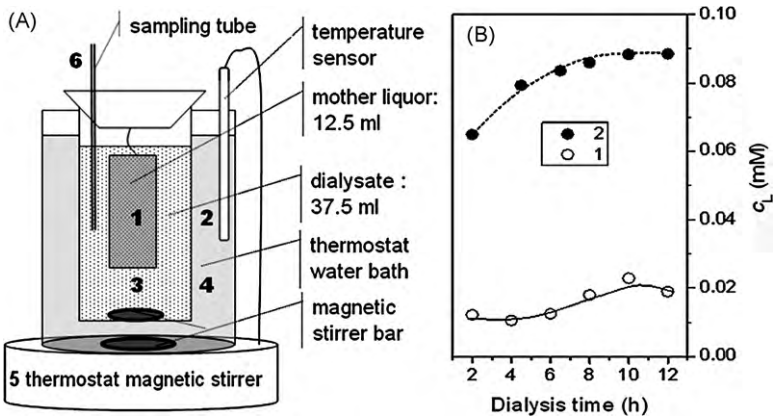

Fig. 1. (A) The device designed for equilibrium dialysis. (B) Effect of dialysis time on recovery of BPA and AA in the mother liquor containing: 1–0.08 mmol/L BPA and 2–0.40 mmol/l AA at pH 7.4 in 0.15 mol/l NaCl.

DNA in order to reveal the comparative toxicity from molecular structure.

2. Material and methods

2.1. Instruments and materials

A Model F-4500 fluorospectrophotometer (Hitachi High-Technology, Tokyo, Japan) was used for determination of BPA and fluorescence measurement of BPA–BSA, BPA–DNA solutions. A Model Lambda-25 spectrometer (Perkin-Elmer, USA) was used to determine the AA concentration during the equilibrium dialysis. The Isothermal Titration Calorimeter (ITC) experiments were carried out on a Model VP-ITC system (MicroCal, USA). A Model J-715 CD spectropolarimeter (Jasco Instruments, Tokyo, Japan) with secondary structure estimation-standard analysis software was used to determine the conformation of BSA and DNA. The Model RC 30–5K semi-permeable membranes (Molecular Weight Cut Off 5 kDa, Shanghai Green Bird STD, China) were used for equilibrium dialysis.

0.100 mmol/l BSA (Sigma, A7906) and 3.7 mmol/l DNA-P (P: phosphorus content) (Shanghai Chemical Reagents, China) were prepared in deionized water as a stock solution. The precise concentration of protein and DNA was determined by UV. 0.400 mmol/l BPA and 100 mmol/l AA were prepared by dissolving BPA and AA (purity 99%, Sigma–Aldrich Reagents) in deionized water. 0.1276 mmol/l vitamin B_2 (VB_2) was prepared by dissolving vitamin B_2 (purity 99%, Shanghai Chemical Reagents, China) in deionized water. The above solutions were all stored at 4 °C. A Britton–Robinson (B–R) buffer (pH 7.4) containing 0.040 mol/l phosphoric acid, acetic acid and boric acid was used.

2.2. Determination of BPA and AA

All studied were carried out in a 10-ml calibrated flask containing 2 ml B–R buffer and a known volume of 0.400 mmol/l BPA or 100 mmol/l AA. The solution was diluted to 10.0 ml with deionized water and mixed thoroughly. After 5 min at room temperature, the fluorescence intensity of BPA solutions were measured at the excitation wavelength (λ_{ex} 277 nm) and the emission wavelength (λ_{em} 306 nm) by fluorospectrophotometry and the absorbance of AA solution at 220 nm with spectrophotometer.

2.3. Dialysis assay of the BPA/AA–BSA/DNA interactions

A schematic diagram of equilibrium dialysis was shown in Fig. 1A. To find equilibrium dialysis time of BPA or AA solutions, 12.5 ml of solution containing 2.5 ml of B–R buffer, 0.15 mol/l NaCl, a known volume of BPA or AA and deionized water was pipeted into dialysis bags (1). 37.5 ml of the dialysate solution containing 0.15 mol/l NaCl, 7.5 ml of B–R buffer and deionized water was added to the dialysis cup (3). The temperature (2) of the water bath (4) was kept constant at 25 °C by adjusting the thermostat magnetic stirrer (5). 2.5 ml of the dialysis solution (3) was collected every 2 h from the sampling tube (6) and the concentration of BPA or AA was determined by the above spectrophotometric method until equilibrium dialysis was confirmed to have been attained at 10 h (Fig. 1B). Then several dialyses containing varying concentrations of BPA or AA solutions were conducted continuously for 10 h and concentrations of BPA or AA were measured once at the end of the equilibration period, 10 h. Thus, the standard curve of BPA or AA for equilibrium dialysis was made for correction of BPA or AA loss resulting from the absorption of semi-permeable membranes. For characterization of the BPA/AA with BSA/DNA interactions, B–R buffer, NaCl, a known volume of BSA or DNA solution (c_{M0}) and a known BPA or AA (c_{L0}) were added in dialysis bags (1). The water bath (4) was kept at 37 °C. Using the same method, the equilibrium dialysis of BPA or AA with BSA or DNA was confirmed to be attained at 10 h, too. 2.5 ml of the dialysis solution (3) was collected and the concentrations of BPA or AA (c_L) determined. The binding ratio (γ) of BPA or AA was calculated by the relation [50].

$$\gamma = \frac{c_{L0} - 4c_L}{c_{M0}} \quad (1)$$

2.4. Fluorescence measurement of the BPA–BSA/DNA solutions

The B–R buffer (2.00 ml) and 0.400 ml of 0.100 mmol/l BSA were mixed with 0–144 μmol/l of BPA. The solutions were diluted to 10 ml with deionized water and their fluorescence intensities were measured at 280 nm (λ_{ex}) and 250–450 nm (λ_{em}). Using the same method, 2.5 ml of 0.400 mmol/l BPA were mixed with 0–0.280 μmol/l BSA or 0–0.290 mmol/l DNA-P, respectively. Their fluorescence intensities were measured at 277 nm (λ_{em}) and 306 nm (λ_{ex}) and the fluorescence intensity corrected by a BSA solution without BPA.

2.5. ITC characterization of the BPA/AA–BSA/DNA interactions

ITC experiments were carried out as follows. The BPA solution (0.250 mmol/l) or AA solution (2.50 mmol/l) was injected about 27 times in 10-μl increments at 270-S intervals into the isothermal cell containing BSA (0.002 or 0.010 mmol/l) or DNA-P (0.050 or 0.500 mmol/l). The cell temperature was kept at 37 °C. In each experiment, an exothermic heat pulse was detected follow-

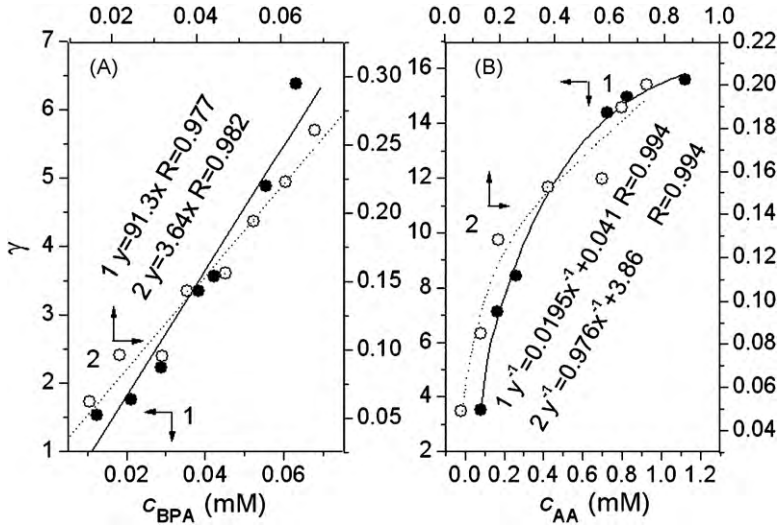

Fig. 2. Plots of γ versus c_L for the BPA/AA–BSA/DNA solutions at pH 7.4 and 37 °C in 0.15 mol/l NaCl. (A) BPA solutions contained 0.02 mmol/l BSA (1) and 0.34 mmol/l DNA-P (2). (B) AA solutions contained 0.02 mmol/l BSA (1) and 0.67 mmol/l DNA-P (2).

ing every injection. Its magnitude progressively decreases until a plateau is reached indicating the saturation of binding. The heat involved at each injection was corrected for the heat of dilution, which was determined separately by injecting the BPA or AA solution into the B–R buffer and then divided by the number of moles injected and then analyzed. The N, enthalpy change (ΔH), and entropy change (ΔS) of the reaction were calculated by the Gibbs free energy (ΔG) equation

2.6. CD measurement of BSA and DNA

The B–R buffer (1 ml), 0.04 ml BSA (0.100 mmol/l) were mixed with 0, 4.80, 8.00 μmol/l BPA or 0, 32, 100 μmol/l AA in three flasks .The solutions were diluted to 10.0 ml with deionized water. Each sample was allowed to equilibrate for 15 min before measurement. CD spectra were taken on a spectropolarimeter with a 0.1 cm light path cell at 25 °C. The mean residue ellipticity (θ) of BSA was measured between 190 and 250 nm. From θ curves, the relative contents of secondary structure forms of BSA including α-helix, β-pleated sheet, β-turn and random coil, were calculated. The 110 μmol/l DNA-P containing 0, 53 and 67 μmol/l BPA and 84 μmol/l DNA-P containing 0, 20 and 70 μmol/l AA were measured with the same method.

2.7. Effects of BPA and AA on the physiological function of BSA

The fluorescence of VB_2 was measured at 440 nm (λ_{ex}) and 525 nm (λ_{em}) with fluorospectrophotometer. The equilibrium dialysis for VB_2 as well as that for VB_2–BSA solution was confirmed to be attained at 10 h, too. The VB_2 standard curve for equilibrium dialysis was made at 25 °C in the same way as that of BPA introduced above.

Concerning the effects of BPA and AA on the BSA's physiological function, i.e., transport VB_2, 12.5 ml of a solution containing 2.5 ml of B–R buffer, 0.15 mol/l NaCl, 0.02 mmol/l BSA, 0.041 mmol/l VB_2 and a known BPA or AA were pipeted into dialysis bags (Fig. 1A-1). After dialysis for 10 h at 37 °C, 2.5 ml of the dialysis solution (Fig. 1A-3) was collected and the VB_2 concentration determined. The binding number of VB_2 was calculated.

3. Results and discussion

3.1. Characterization of the BPA/AA–BSA/DNA interactions

By measuring a series of BPA or AA solutions containing known concentrations of BSA and DNA, γ was calculated. The Pesavento partition and Langmuir isothermal models were used to fit the experimental data [51].

$$\gamma = K_{ow} \times c_L \tag{2}$$

and

$$\frac{1}{\gamma} = \frac{1}{N} + \frac{1}{KNc_L} \tag{3}$$

where K_{ow} is the partition coefficient, and K the adsorption constant. By regressing plots of γ versus c_L, all plots are shown in Fig. 2. The good linear relationships indicated that the bindings of BPA and AA to peptide chains and DNA duplex obeyed the two models above. It indicates that the more BPA is added, the more BPA will bind to BSA and DNA. Therefore, there will be no saturation during the BPA binding process.

γ (Fig. 2B) approaches the following maximum: 16 for AA binding to BSA (curve 1) and 0.2 for AA to DNA-P (curve 2). From the intercepts and gradients of the regression lines (Fig. 2B), N of AA was calculated to be 24 per mol BSA and 0.26 per mol DNA-Py. The binding of AA to BSA and DNA obeyed the Langmuir isothermal model so the interactions of AA with BSA and DNA responds to a chemical monolayer adsorption.

In common, electrostatic attraction plays an important role in the binding of ligands to protein. Concerning the drug-binding mechanism of DNA, the binding of distamycin to DNA is associated with electrostatic interaction [47]. However, this is not the case in this study. From the dissociation constants (K_R) of the side groups (R) of basic and acidic amino acid residues (AARs) of BSA (K_R = 10.53 for Lys, 6.00 for His, 12.48 for Arg, 3.65 for Asp, and 4.25 for Glu), only the side groups of Lys and Arg residues will be protonated and positively charged in neutral media. Therefore, electrostatic attraction cannot be the main contributor. The hydrophobic stack, e.g., π–π accumulation, will be formed between the benzene ring of BPA and many aromatic residues (Phe, Tyr and Trp) of BSA. In addition, the $-NH_2$ of AA have affinity for the polar amino acid residues of BSA and G, T and A bases of DNA duplex. Thus, hydrogen bonds,

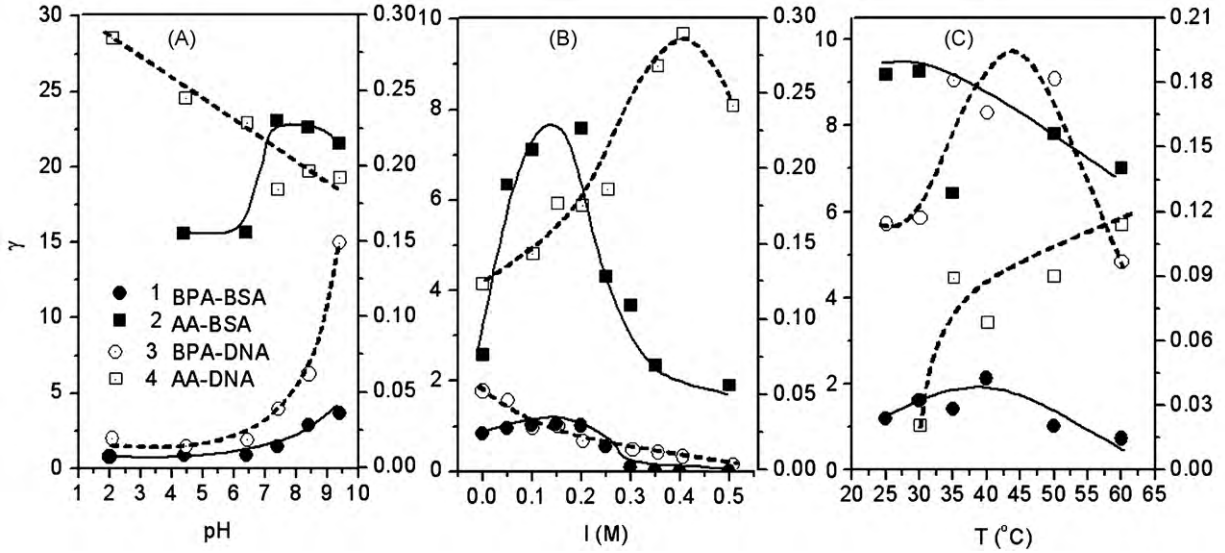

Fig. 3. Effects of pH (A), electrolyte (B) and temperature (C) on γ. Solutions contained: 1–0.02 mmol/l BSA and 0.192 mmol/l BPA (A and C) and 0.144 mmol/l BPA (B); 2–0.02 mmol/l BSA and 2.4 mmol/l AA; 3–0.36 mmol/l DNA-P (A and C) and 0.24 mmol/l BPA (A and C), 0.18 mmol/l DNA-P (B) and 0.14 mmol/l BPA (B); 4–0.8 mmol/l AA and 0.67 mmol/l DNA-P.

e.g., N···H···N and N···H···O may be formed when AA interacts with BSA and DNA.

3.2. Effects of pH, electrolyte and temperature

The stability of non-covalent interaction is always affected by pH, ionic strength and temperature [52,53]. With increasing pH, γ for BPA–BSA/DNA and AA–BSA increases whereas that for AA–DNA decreases (Fig. 3A). It implies that the acidic media are more favorable for AA binding to DNA. Concerning the isoelectric point of DNA at pH 4–4.5, it is more likely that H-bonds are formed between $-NH_2$ of AA and C=O, =N– of DNA's bases. Moreover, several $-NH_2$ groups of AA will be positively charged in acidic media, which is favorable for the electrostatic attraction between the negative phosphate group and $-NH_2^+$ of AA. This is probably another reason that γ for the AA–DNA interaction increases in acidic media. However, in neutral and alkali media DNA turns to be anions and the attack to nucleophilic groups of bases by $-NH_2$ of AA is inhibited to some degree, possibly affecting the formation of H-bonds and leading to the decrease of γ. From γ in alkali media, there may be hydrophobic effect between AA and DNA.

From Fig. 3B, γ of BPA decreases with increasing sodium chloride while that of AA increases obviously and then decreases. γ for BSA–BPA/AA reaches the maximum at 0.15 mol/l sodium chloride, implying that the normal physiological condition is favorable for transmission of endogenous pollutants by serum albumin. γ for DNA–AA approaches the maximum at 0.4 mol/l sodium chloride, indicating the increase of ionic strength is favorable for AA bind-

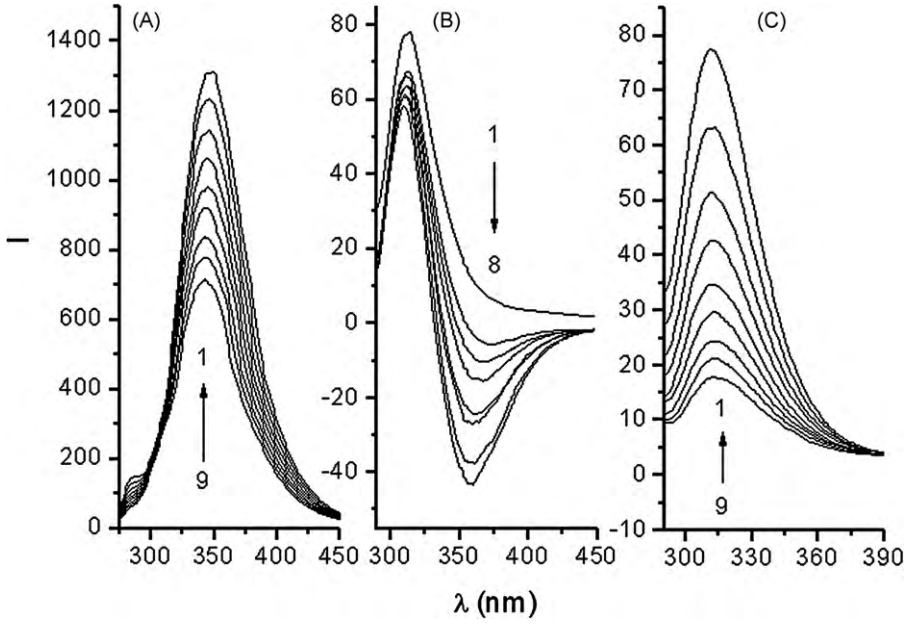

Fig. 4. The fluorescence spectra of the BSA–BPA (A and B) and DNA–BPA (C) solutions at pH 7.4. (A) 4 μmol/l BSA and variable BPA (curve 1–9): 0, 18, 36, 54, 72, 90, 108, 126 and 144 μmol/l. (B) 0.1 mmol/l BPA and variable BSA (curve 1–8): 0.00, 0.04, 0.08, 0.12, 0.16, 0.20, 0.24 and 0.28 μmol/l. (C) 0.1 mmol/l BPA and variable DNA-P (curve 1–9): 0.000, 0.037, 0.073, 0.110, 0.146, 0.180, 0.220, 0.260 and 0.290 mmol/l.

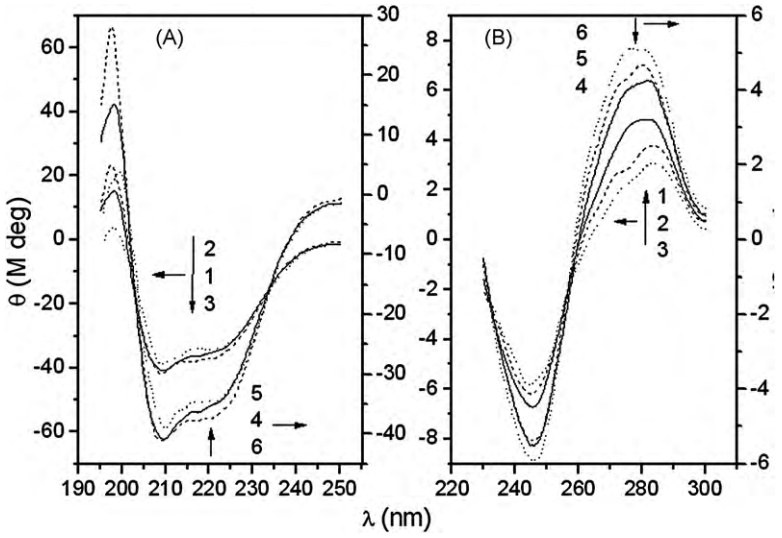

Fig. 5. The molar ellipticity CD spectra of the AA/BPA–BSA/DNA solutions: (A) 0.4 μmol/l BSA containing BPA (curve 1–3): 0, 4.8, 8.0 μmol/l and AA (curve 4–6): 0, 32 and 100 μmol/l; (B) 110 μmol/l DNA-P containing BPA (curve 1–3): 0, 53 and 67 and 84 μmol/l DNA-P containing AA (curve 4–6): 0, 20, and 70 μmol/l. All solutions were at pH 7.4.

ing to DNA. Moreover, the involvement of Na^+ in the interaction of the phosphate group did not have much effect on AA binding to DNA. It implies that electrostatic attraction is not the main force that connects AA to DNA.

High temperature often affects on non-covalent interactions [54]. Frpom Fig. 3C, γ reaches the maximum at about 40 °C for BPA solutions. It indicates that the normal physiological conditions (37 °C) may be favorable for the binding of BPA. γ for BPA–BSA changes slightly with heating, which may result from the combination of the hydrophobic interaction and H-bond formed between BPA and the peptide chain. In contrast, γ for AA–BSA decreased while that for AA–DNA increased obviously. Temperature increase will lead to the increase of distance between the peptide chain and organic molecules, which may help the increase of γ for AA–BSA.

3.3. Identification of target amino acid residues

Serum albumin contains Trp, Phe and Tyr residues and its intrinsic fluorescence intensity depends on the degree of exposure of these residues to the polar, aqueous solvent and their proximity to specific quenching groups such as protonated carboxyl, protonated imidazole and deprotonated ε-amino groups [55]. Two models have been proposed for the quenching of protein fluorescence, static quenching and synthetic dynamic quenching [56]. The classical relation, i.e., Stern–Volmer equation often employed to describe the collisional (dynamic) quenching process:

$$\frac{F_0}{F} = 1 + K_q \tau_0 [Q] \quad (4)$$

where F_0 is the fluorescence intensity of BSA, F that of BSA in the presence of AA or BPA, τ_0 the lifetime of BSA at 10^{-8} s [Q] the AA or BPA concentration and K_q the quenching rate constant at 2.0×10^{10} l/(mol s) as the highest limit for dynamic quenching. In static quenching, the quencher will bind to Phe, Tyr, especially Trp residues of BSA, change the microenvironments of these residues and even alter the secondary structure of BSA. The fluorescence spectra of BSA and BPA with the addition of BPA and BSA were obtained (Fig. 4), respectively. From Fig. 4A, a gradual decrease in the fluorescence intensity of BSA was observed accompanied by a slight blue shift (6 nm) in the emission wavelength, which indicated BPA bound to Trp (W) residues and the microenvironment around Trp (W), Phe (F) and Tyr (Y) residues in BSA was changed consequently. Thus, interaction between BPA and BSA result in static quenching of the intrinsic protein fluorescence, especially that of Trp residue, W214 of BSA. This was confirmed by the fluorescence spectra of BPA quenched by BSA shown in Fig. 4B. Slight blue shift was also observed along with the decreasing in the fluorescence spectra of BPA, the trough of which provides strong evidence of BPA–BSA static quenching again. BSA contains three hydrophobic cavities and all hydrophobic amino acid residues were present there and their hydrophobic environment is favorable for organic molecule to enter there [57]. When interacting with BSA, BPA may enter these cavities and interact with amino acid residues, especially with Trp, via hydrophobic π–π stack formed between the benzene ring of BPA and aromatic hydrocarbon groups of BSA such as Phe, Tyr and Trp.

The Stern–Volmer equation can also be applied for the fluorescence quenching of BPA by DNA (Fig. 4C). The fluorescence intensity of BPA decreased with the addition of DNA, but no wavelength shift was observed. This indicates that BPA binds to DNA by intercalating between adjacent basepairs of DNA and π–π stack is enhanced consequently, although the interaction between BPA and DNA is weaker than that of BPA and BSA.

3.4. Variation of the secondary conformation of BSA and DNA

When organic compounds such as pollutants, drugs or toxicants interact with protein or DNA, the internal non-covalent bonds of the peptide chain or DNA duplex are often disrupted, possibly changing the original conformation or even their special function. CD spectrometry is often used to evaluate the secondary structure of DNA [44] and protein [48]. From CD spectra of the BPA/AA–BSA/DNA solutions (Fig. 5), the fractions of β-pleated sheet, α-helix, β-turn and random forms were calculated (Table 1). With the addition of BPA or AA, the CD spectra of BSA changed obviously. The β-pleated sheet fraction of BSA decreases from 20.2% to 0%, whereas the α-helix and β-turn content increases from 22.8% to 27.7% and 26.5% to 34.5%, respectively, in the presence of AA. Similarly, with the addition of BPA, BSA secondary structure changes from 20.2% β-pleated sheet down to only 4% and 22.8% α-helix up to 27.3% and 26.5% β-turn to 32.8%. Obviously the disappearance of β-pleated sheet results in the increase of α-helix and β-turn content. Although the non-covalent bonds between BPA/AA and BSA in neutral solution are weaker than that in acidic solution [58,59], the addition of BPA

Table 1
Change of the secondary structure of BSA (0.4 μmol/l) in the presence of AA and BPA at pH 7.4 (n = 3).

Factor	BSA	BPA (μmol/l)		AA (μmol/l)	
		4.8	8	32	100
α-Helix (%)	22.8 ± 2.2%	25.9 ± 1.9%	27.3 ± 2.4%	25.6 ± 1.2%	27.7 ± 1.2%
β-Pleated sheet (%)	20.2 ± 2.5%	16.9 ± 2.4%	4 ± 3.5%	17.7 ± 1.4%	0
β-Turn (%)	26.5 ± 3.0%	27.5 ± 1.5%	32.8 ± 2.3%	26.4 ± 2.3%	34.5 ± 2.3%
Random coil (%)	30.5 ± 3.1%	29.7 ± 1.7%	35.9 ± 1.8%	30.3 ± 2.0%	37.7 ± 3.0%

or AA causes obvious secondary conformation change in BSA. The addition of BPA or AA transforms some β-pleated sheet into α-helix and β-turn.

The CD spectra of DNA show a signal characteristic of a B-form helix with a negative band at 245 nm and a positive band at 275 nm. The decrease in band amplitudes at 275 nm (Fig. 5B 1–3) and slight change of the shape of the positive band were observed upon addition of BPA, which indicates BPA binds to DNA by intercalating between adjacent basepairs and induces a conformational change of DNA. In contrast, the enhancement of CD spectra at 275 nm (Fig. 5B 4–6) in the presence of AA and shape change of the positive band suggest AA binds to the minor groove of DNA, resulting from the combination of H-bonds formed between –NH of AA and nucleophilic nitrogen or oxygen atom of A, T, G bases of DNA and hydrophobic π–π interactions via vinyl groups.

3.5. Thermodynamic characterization of the BPA/AA–BSA/DNA interactions

From Fig. 6, all ΔH are much less than 60 kcal/mol [60] so the BPA/AA–BSA/DNA interactions are non-covalent, involving hydrogen bond, hydrophobic effect, e.g., π–π stack, dispersion force and van der Waals force. Moreover, all the reactions are driven by entropy change and thus spontaneous on account of the conformational change of biomolecules induced by the reactions.

From Fig. 6A and C, the heat released from the BPA–BSA/DNA interactions exhibits a saltatory decrease toward 0. It indicates that BPA binding is affected easily by the dilution and mixing of the solutions, which result in the weak binding of BPA and subsequent dissociation of BPA from BSA or DNA. The impossibility for BPA binding to reach a plateau indicates the occurrence of hydrophobic interactions between BPA and aromatic hydrocarbon groups (Phe, Tyr and Trp) of BSA and consequent partition mode of BPA binding. On the contrary, the heat released from both AA–BSA (Fig. 6B) and AA–DNA (Fig. 6D) interactions approaches 0 when $c_{L0}/c_{M0} > 15$ and 0.3, respectively, implying the plateau is being reached. Therefore, AA binds to BSA and DNA via H-bonds.

On account of the three-dimensional conformation of BSA, it's very likely that the binding modes for AA–BSA are on the surface (N_i = 8) and inside the cavity (N_i = 15). First, AA binds to the BSA surface via H-bonds between C=O, $-NH_2$ of AA and many polar residues of BSA. The reaction is exothermic. After the binding sites of BSA surface have been occupied, AA enters the cleft of BSA easily. So the inside binding is endothermic. Due to the small cavity where the inside binding occurs and consequent effect on BSA conformation, entropy change is much more obvious than that of outside binding. It indicates BSA conformation is changed due to AA binding.

According to the thermal dynamic parameters, the binding of AA to DNA-P probably also respond to a two-step sequential interaction: minor groove binding (N_i = 0.1) and major groove binding

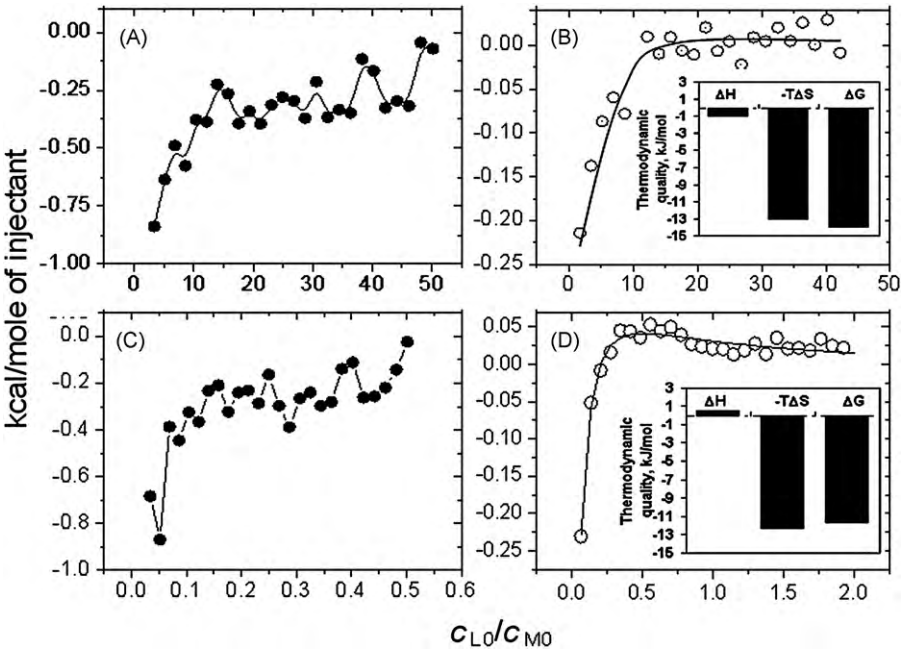

Fig. 6. ITC titration curves of (A) BPA–BSA, (B) AA–BSA, (C) BPA–DNA, (D) AA–DNA interactions at pH 7.4 and 37 °C (n = 3, RSD = 1.0%, 1.4%, 1.2% and 1.6%). The experiment was conducted by injecting (10 μl every time): (A and C) 0.25 mmol/l BPA into the ITC cell (1.4685 ml) containing (A) 0.002 mmol/l BSA or (C) 0.05 mmol/l DNA-P, and (B and D) 2.5 mmol/l AA into the ITC cell (1.4685 ml) containing (B) 0.01 mmol/l BSA or (D) 0.5 mmol/l DNA-P. The titration profile was integrated and corrected for the heat of dilution, which was estimated by a separate experiment by injecting the BPA or AA into the B–R buffer. The corrected heat was divided by the moles of injectant, and values were plotted as a function of the BPA–BSA, AA–BSA, BPA–DNA, AA–DNA molar ratio. The titration curve was fitted by a nonlinear least squares method.

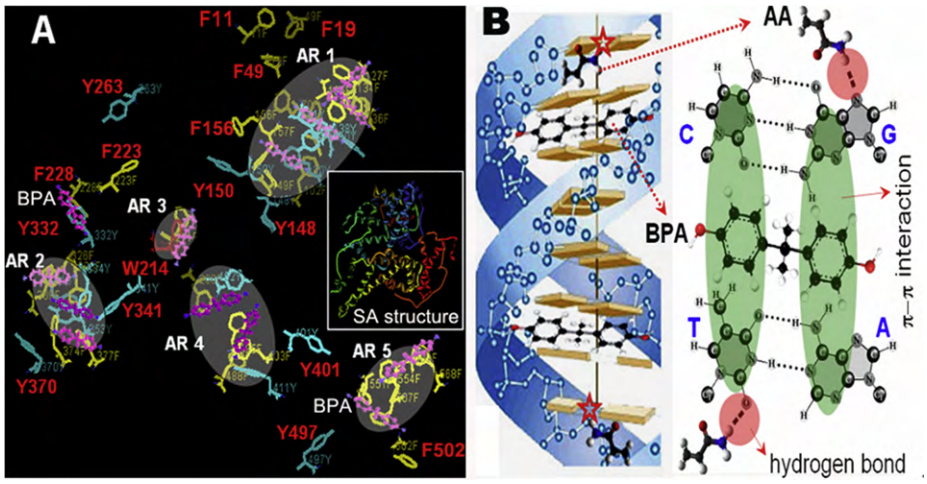

Fig. 7. Cartoon illustrating the possible binding sites of BPA and AA in BSA (A) and DNA (B).

(N_i = 0.15). The ΔH value integrated in the first step is almost the same as that of $-T\Delta S$. It suggests that the reaction was driven by both ΔH and ΔS, accompanied by the formation of H-bonds [48,44], which are the most likely groups, e.g., $-NH_2$ of AA and nucleophilic nitrogen or oxygen atom of A, T and G bases of DNA such as C=O, –N=C, and the hydrophobic interaction. In the second step, both ΔH and ΔS are positive. Therefore, the reaction was driven by ΔS, which may result from the hydrophobic stack of AA binding in DNA groove and the conformation change of DNA duplex. The binding process may be accompanied by the electrostatic interaction between AA and the phosphate group of DNA. Moreover, the fact that ΔH is positive when c_{L0}/c_{M0} is 1:1 indicates that the reaction is endothermic and the increase of temperature is favorable for the interaction, which is in agreement with the result of equilibrium dialysis. In short, Minor groove binding is comparatively firmer while major groove binding is weaker.

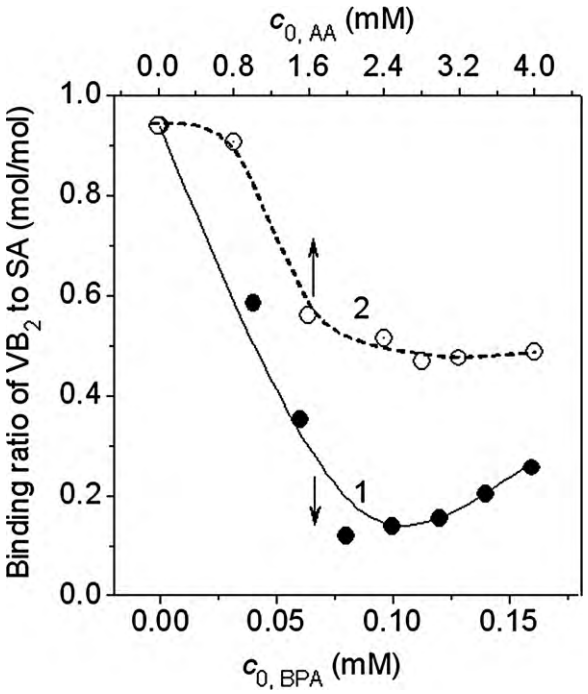

Fig. 8. Effect of BPA (1) and AA (2) on the physiological function of BSA to transport VB_2. All solutions contained 0.02 mmol/l BSA and 0.04 mmol/l VB_2 at pH 7.4 and 37 °C in 0.15 mol/l NaCl.

3.6. Binding illustration

Fig. 7 illustrates that both BPA and AA interact with BSA and DNA. There are altogether 5 aromatic residues (Phe, Tyr and Trp) regions (AR) where hydrophobic stack can be formed between BPA and BSA (Fig. 7A), including AR1, AR2, AR3, AR4 and AR5 that consist of many F and Y. AR1 (F70, 127, 165, 134, 157, 102 and 149 and Y30, 161, 138 and 140), AR2 (F309, 326, 374 and 377 and Y334, 341, 319 and 353) and AR5 (F511, 507, 509 and 568) distributed on the external surface of BSA. After that, BPA enters the cavity of BSA and interacts with the aromatic residues of AR3 (F211 and W214) and AR4 (F395, 206, 403 and 488 and Y192 and 411). In a high concentration media, BPA not only interacts with Phe, Tyr and Trp via hydrophobic stack, but also accumulates in AR1–AR5 regions. Thus, more and more BPA molecules bind to BSA. Therefore, BPA interacts with BSA in a partition mode. Because the aromatic amino acids are covered up by hydrophobic stacking, especially by the interaction of BPA with Trp, W214, the intrinsic fluorescence of BSA quenched (Fig. 4A) obviously whereas that of BPA decreases slightly (Fig. 4B) due to the high ratio (>70%, Fig. 2A) of BPA. Similar to the interaction with BSA, BPA intercalates parallel between adjacent basepairs of DNA, resulting in hydrophobic stack (Fig. 7B). With increase of BPA, a super hydrophobic region where hydrophobic groups gather is formed in the center of DNA duplex. Because of the intercalation of BPA with basepairs of DNA, the CD spectra of DNA was reduced and the fluorescence intensity of BPA decreases obviously in the presence of DNA because of BPA hydrophobic stacking.

In contrast, AA can interacts with various polar amino acid residues of BSA via H-bond owing to its high polarity. When interacting with G, T and A bases and gathering in the major and minor groove of DNA duplex, AA runs parallel with the side chain of DNA, resulting in the more disperse electron clouds of basepairs and consequent enhancement of CD spectra of DNA, which is contrary to that of BPA–DNA.

3.7. Effects of BPA and AA on the physiological function of BSA

The relationship between structural transformation of protein and its functioning is of great significance in organisms. During interaction process, a small organic compound may bind to the peptide chain, regulating its three-dimensional structure and even changing its corresponding function [61–62]. Although non-covalent binding is often weak and non-specific, a combination of many non-covalent bonds may alter the conformation and function of the protein [63]. Serum albumin is the major plasma carrier

protein in blood [1–3,7–9]. It is responsible for the maintenance of both the oncotic pressure and the pH of blood [4,64]. The effects of BPA and AA on BSA function to transport VB_2 were illustrated in Fig. 8. With the addition of BPA and AA, the binding ratio of VB_2 to BSA decreases obviously. It indicates the inhibition of BSA carriage capacity by the pollutants. At the normal physiological condition, 0.100 mmol/l BPA reduces the binding ratio of VB_2 to BSA by more than 70%, and 2.8 mmol/l AA by almost one half. This could be attributed to the competition of VB_2 binding sites in BSA by pollutants. Therefore, non-covalent binding of the organic compound severely affects the physiological function of protein.

4. Conclusions

The interactions of BPA and AA with BSA and DNA were characterized using various methods and important results obtained concerning, e.g., binding number, binding energy, and type of binding. The interactions above obeyed the Pesavento partition and Langmuir isothermal models, respectively. The saturation binding numbers of AA were calculated to be 24 on BSA and 0.26 on DNA-P. All the reactions are driven by entropy change and spontaneous. Hydrophobic effect is the main contributor that induce BPA binding to BSA and the intercalation of BPA between adjacent basepairs of DNA duplex. And hydrogen bond promotes the interaction of AA with BSA and groove binding of AA to DNA. The secondary structure of both BSA and DNA changed in the presence of BPA and AA, with the binding ratio of VB_2 to BSA being reduced by more than 70% and almost one half, indicating that the transport function of BSA was inhibited consequently.

Acknowledgments

The authors thank both the Key Laboratory Foundation of Education Ministry of China (Grant No. YRWEY 1008) and the National Basic Research Program of China (973) (Grant No. 2010CB912604) for financially supporting this work.

References

[1] J.K. Choi, J. Ho, S. Curry, D.H. Qin, R. Bittman, J.A. Hamilton, Interactions of very long-chain saturated fatty acids with serum albumin, J. Lipid Res. 43 (2002) 1000–1010.
[2] I.N. Bojesen, E. Bojesen, Binding of arachidonate and oleate to bovine serum albumin, J. Lipid Res. 35 (1994) 770–778.
[3] J.A. Hamilton, S. Era, S.P. Bhamidipati, R.G. Reed, Locations of the three primary binding sites for long-chain fatty acids on bovine serum albumin, Proc. Natl. Acad. Sci. U.S.A. 88 (1991) 2051–2054.
[4] N. Shakai, R.L. Garlick, H.F. Bunn, Nonenzymatic glycosylation of human serum albumin alters its conformation and function, J. Biol. Chem. 259 (1984) 3812–3817.
[5] A.A. Bhattacharya, S. Curry, N.P. Franks, Binding of the general anesthetics propofol and halothane to human serum albumin: high-resolution crystal structures, J. Biol. Chem. 275 (2000) 38731–38738.
[6] P.A. Zunszain, J. Ghuman, T. Komatsu, E. Tsuchida, S. Curry, Crystal structural analysis of human serum albumin complexed with hemin and fatty acid, BMC Struct. Biol. 3 (2003) 6.
[7] I. Petitpas, A.A. Bhattacharya, S. Twine, M. East, S. Curry, Crystal structure analysis of warfarin binding to human serum albumin, J. Biol. Chem. 276 (2001) 22804–22809.
[8] T.G. Burk, Z. Mi, The structural basis of camptothecin interactions with human serum albumin: impact on drug stability, J. Med. Chem. 37 (1994) 40–46.
[9] J.T. Rhule, C.L. Hill, D.A. Judd, R.F. Schinazi, Polyoxometalates in medicine, Chem. Rev. 98 (1998) 327–358.
[10] M. Purcell, J.F. Neault, H. Malonga, H. Arakawa, R. Carpentier, H.A. Tajmir-Riahi, Interaction of atrazine and 2,4-D with human serum albumin studied by gel and capillary electrophoresis, and FTIR spectroscopy, Biochim. Biophys. Acta 1548 (2001) 129–138.
[11] V. Berger, A.F. Gabriel, T. Sergent, A. Trouet, Y. Larondelle, Y.J. Schneider, Interaction of ochratoxin A with human intestinal Caco-2 cells: possible implication of a multidrug resistance-associated protein (MRP2), Toxicol. Lett. 140 (2003) 465–476.
[12] D. Silva, C.M. Cortez, J. Cunhua-Bastos, S.R. Louro, Methyl parathion interaction with human and bovine serum albumin, Toxicol. Lett. 147 (2004) 53–61.
[13] S.J. Uddin, J.A. Shilpi, G.M. Murshid, A.A. Rahman, M.M. Sarder, M.A. Alam, Determination of the binding sites of arsenic on bovine serum albumin using warfarin (site-I specific probe) and diazepam (site-II specific probe), J. Biol. Sci. 4 (2004) 609–612.
[14] D. Svozil, J. Kalina, M. Omelka, B. Schneider, DNA conformations and their sequence preferences, Nucleic Acids Res. 36 (2008) 3690–3706.
[15] K.D. Goodwin, M.A. Lewis, E.C. Long, M.M. Georgiadis, Crystal structure of DNA-bound Co(III)·bleomycin B_2: insights on intercalation and minor groove binding, Proc. Natl. Acad. Sci. U.S.A. 105 (2008) 5052–5056.
[16] F. Barcelo, C. Scotta, M. Ortiz-Lombardia, C. Mendez, A.J. Salas, J. Portugal, Entropically-driven binding of mithramycin in the minor groove of C/G-rich DNA sequences, Nucleic Acids Res. 35 (2007) 2215–2226.
[17] B.I. Ghanayem, L.P. McDaniel, M.I. Churchwell, N.C. Twaddle, R. Snyder, T.R. Fennell, D.R. Doerge, Role of CYP2E1 in the epoxidation of acrylamide to glycidamide and formation of DNA and hemoglobin adducts, Toxicol. Sci. 88 (2005) 311–318.
[18] A. Adeeko, D. Li, J. Doucet, G.M. Cooke, J.M. Trasler, B. Robaire, B.F. Hales, Gestational exposure to persistent organic pollutants: maternal liver residues, pregnancy outcome, and effects on hepatic gene expression profiles in the dam and fetus, Toxicol. Sci. 72 (2003) 242–252.
[19] R. Baliga, D.M. Crothers, On the kinetics of distamycin binding to its target sites on duplex DNA, Proc. Natl. Acad. Sci. U.S.A. 97 (2000) 7814–7818.
[20] Y. Kamei, H. Ohizumi, Y. Fujitani, T. Nemoto, T. Tanaka, N. Takahashi, T. Kawada, M. Miyoshi, O. Ezaki, A. Kakizuka, PPARγ coactivator 1/βERR ligand 1 is an ERR protein ligand, whose expression induces a high-energy expenditure and antagonizes obesity, Proc. Natl. Acad. Sci. U.S.A. 100 (2003) 12378–12383.
[21] T. Hiroi, K. Okada, S. Imaoka, M. Osada, Y. Funae, Bisphenol A binds to protein disulfide isomerase and inhibits its enzymatic and hormone-binding activities, Endocrinology 147 (2006) 2773–2780.
[22] H.H. Le, E.M. Carlson, J.P. Chua, S.M. Belcher, Bisphenol A is released from polycarbonate drinking bottles and mimics the neurotoxic actions of estrogen in developing cerebellar neurons, Toxicol. Lett. 176 (2008) 149–156, 2.
[23] A. Takahashi, F. Higashino, M. Aoyagi, S. Kyo, T. Nakata, M. Noda, M. Shindoh, T. Kohgo, H. Sano, Bisphenol A from dental polycarbonate crown upregulates the expression of hTERT, J. Biomed. Mater. Res. 71B (2004) 214–221.
[24] International Agency for Research on Cancer (IARC), IARC Monographs on the Evaluation of the Carcinogenic Risk of Chemicals to Humans: Some Industrial Chemicals, vol. 60, International Agency for Research on Cancer (IARC), Lyon (France), 1994, pp. 389–443.
[25] Y. Sugita-Konishi, S. Shimura, T. Nishikawa, F. Sunaga, H. Naito, Y. Suzuki, Effect of bisphenol A on non-specific immunodefenses against non-pathogenic *Escherichia coli*, Toxicol. Lett. 136 (2003) 217–227.
[26] D.C. Dolinoy, D. Huang, R.L. Jirtle, Maternal nutrient supplementation counteracts bisphenol A-induced DNA hypomethylation in early development, Proc. Natl. Acad. Sci. U.S.A. 104 (2007) 13056–13061.
[27] J.C. Kim, H.C. Shin, S.W. Cha, W.S. Koh, M.K. Chung, S.S. Han, Evaluation of developmental toxicity in rats exposed to the environmental estrogen bisphenol A during pregnancy, Life Sci. 69 (2001) 2611–2625.
[28] P. Sohoni, C.R. Tyler, K. Hurd, J. Caunter, M. Hetheridge, T. Williams, C. Woods, M. Evans, R. Toy, M. Gargas, J.P. Sumpter, Reproductive effects of long-term exposure to bisphenol A in the Fathead Minnow (*Pimephales promelas*), Environ. Sci. Technol. 35 (2001) 2917–2925.
[29] S.H. Dairkee, J. Seok, S. Champion, A. Sayeed, M. Mindrinos, W.Z. Xiao, R.W. Davis, W.H. Goodson, Bisphenol A induces a profile of tumor aggressiveness in high-risk cells from breast cancer patients, Cancer Res. 68 (2008) 2076–2080.
[30] T. Niwa, M. Fujimoto, K. Kishimoto, Y. Yabusaki, F. Ishibashi, M. Katagiri, Metabolism and interaction of bisphenol A in human hepatic cytochrome P450 and steroidogenic CYP17, Biol. Pharm. Bull. 24 (2001) 1064–1067.
[31] R.M. LoPachin, The changing view of acrylamide neurotoxicity, Neurotoxicology 25 (2004) 617–630.
[32] A. Besaratinia, G.P. Pfeifer, Weak yet distinct mutagenicity of acrylamide in mammalian cells, J. Natl. Cancer. Inst. 95 (2003) 889–896.
[33] R.W. Tyl, M.A. Friedman, Effects of acrylamide on rodent reproductive performance, Reprod. Toxicol. 17 (2003) 1–13.
[34] C. Martins, N.G. Oliveira, M. Pingarilho, G.G.D. Costa, V. Martins, M.M. Marques, F.A. Beland, M.I. Churchwell, D.R. Doerge, J. Rueff, J.F. Gaspar, Cytogenetic damage induced by acrylamide and glycidamide in mammalian cells: correlation with specific glycidamide–DNA adducts, Toxicol. Sci. 95 (2007) 383–390.
[35] B.I. Ghanayem, K.L. Witt, G.E. Kissling, R.R. Tice, L. Recio, Absence of acrylamide-induced genotoxicity in CYP2E1-null mice: evidence consistent with a glycidamide-mediated effect, Mutation Res. 578 (2005) 284–297.
[36] Q.Y. Xie, H.F. Sun, Y.F. Liu, X.F. Ding, D.P. Fub, K. Liu, Adduction of biomacromolecules with acrylamide (AA) in mice at environmental dose levels studied by accelerator mass spectrometry, Toxicol. Lett. 163 (2006) 101–108.
[37] A. Besaratinia, G.P. Pfeifer, Genotoxicity of acrylamide and glycidamide, J. Natl. Cancer Inst. 96 (2004) 1023–1029.
[38] A. Besaratinia, G.P. Pfeifer, A review of mechanisms of acrylamide carcinogenicity, Carcinogenesis 28 (2007) 519–528.
[39] World Health Organization, FAO/WHO Consultation on the Health Implications of Acrylamide in Food—Summary Report, Geneva, Switzerland, WHO, 2002, pp. 1–12.
[40] D.S. Mottram, B.L. Wedzicha, A.T. Dodson, Acrylamide is formed in the Maillard reaction, Nature 419 (2002) 448–449.
[41] R.H. Stadler, I. Blank, N. Varga, F. Robert, J. Hau, P.A. Guy, M.C. Robert, S. Riediker, Acrylamide from Maillard reaction products, Nature 419 (2002) 449–450.

[42] H.Y. Zhang, I.G. Macara, The PAR-6 polarity protein regulates dendritic spine morphogenesis through p190 RhoGAP and the Rho GTPase, Dev. Cell 14 (2008) 216–226.
[43] S.H. Chen, C.K. Suzuki, S.H. Wu, Thermodynamic characterization of specific interactions between the human Lon protease and G-quartet DNA, Nucleic Acids Res. 36 (2008) 1273–1287.
[44] J. Lah, I. Drobnak, M. Dolinar, G. Vesnaver, What drives the binding of minor groove-directed ligands to DNA hairpins? Nucleic Acids Res. 36 (2007) 897–904.
[45] D.A. Kraut, K.S. Carroll, D. Herschlag, Challenges in enzyme mechanism and energetics, Annu. Rev. Biochem. 72 (2003) 517–571.
[46] X.G. Qu, J.O. Trent, I. Fokt, W. Priebe, J.B. Chaires, Allosteric, chiral-selective drug binding to DNA, Proc. Natl. Acad. Sci. U.S.A. 97 (2000) 12032–12037.
[47] G.L. Olsen, E.A. Louie, G.P. Drobny, S.T. Sigurdsson, Determination of DNA minor groove width in distamycin-DNA complexes by solid-state NMR, Nucleic Acids Res. 31 (2003) 5084–5089.
[48] F.F. Chen, Y.N. Tang, S.L. Wang, H.W. Gao, Binding of brilliant red compound to lysozyme: insights into the enzyme toxicity of water-soluble aromatic chemicals, Amino Acids 36 (2009) 399–407.
[49] W.Y.X. Peh, E. Reimhult, H.F. Teh, J.S. Thomsen, X. Su, Understanding ligand binding effects on the conformation of estrogen receptor a-DNA complexes: a combinational quartz crystal microbalance with dissipation and surface plasmon resonance study, Biophys. J. 92 (2007) 4415–4423.
[50] L.L. Wu, L. Chen, C. Song, X.W. Liu, H.P. Deng, N.Y. Gao, H.W. Gao, Potential enzyme toxicity of PFOA, Amino Acids 38 (2010) 113–116.
[51] M. Pesavento, A. Profumo, Interaction of serum albumin with a sulphonated azo dye in acidic solution, Talanta 38 (1991) 1099–1106.
[52] V. Malkov, O. Voloshin, V.N. Soyfer, M.D. Frank-Kamenetskii, Cation and sequence effects on stability of intermolecular pyrimidine–purine–purine triplex, Nucleic Acids Res. 21 (1993) 585–591.
[53] S.F. Singleton, P.B. Dervan, Temperature dependence of the energetics of oligonucleotide-directed triple-helix formation at a single DNA site, J. Am. Chem. Soc. 116 (1994) 10376–10382.
[54] H.W. Gao, X.H. Liu, Z. Qiu, L. Tan, Non-covalent binding of azo compound to peptide chain resulting in the conformational change of protein: interactions of biebrich scarlet and naphthochrome green with four model proteins, Amino Acids 36 (2009) 251–260.
[55] M. Dockal, D.C. Carter, F. Ruker, Conformational transitions of the three recombinant domains of human serum albumin depending on pH, J. Biol. Chem. 275 (2000) 3042–3050.
[56] G.B. Behera, B.K. Mishra, P.K. Behera, M. Panda, Fluorescent probes for structural and distance effect studies in micelles, reversed micelles and microemulsions, Adv. Colloid Interface Sci. 82 (1999) 1–42.
[57] P.G. Yi, Q.S. Yu, Z.C. Shang, M. Guo, Study on the interaction between chlortetracycline and bovine serum albumin, Chin. J. Chem. Phys. 16 (2003) 420–425.
[58] H.W. Gao, J.F. Zhao, Q.Z. Yang, X.H. Liu, L. Chen, L.T. Pan, Non-covalent interaction of 2′,4′,5′,7′-tetrabromo-4,5,6,7-tetrachlorofluorescein with proteins and its applications, Proteomics 6 (2006) 5140–5151.
[59] H.W. Gao, Q. Xu, L. Chen, S.L. Wang, Y. Wang, L.L. Wu, Y. Yuan, Potential protein toxicity of synthetic pigments: binding of poncean S to human serum albumin, Biophys. J. 94 (2008) 906–917.
[60] M. Yang, Molecular recognition of DNA targeting small molecule drugs, J. Beijing Med. Univ. 30 (1998) 97–99.
[61] M.X. Xie, X.Y. Xu, Y.D. Wang, Interaction between hesperetin and human serum albumin revealed by spectroscopic methods, Biochim. Biophys. Acta 1724 (2005) 215–224.
[62] A. Desai, C. Lee, L. Sharma, A. Sharma, Lysozyme refolding with cyclodextrins, structure–activity relationship, Biochimie 88 (2006) 1435–1445.
[63] B. Piekarska, M. Skowronek, J. Rybarska, B. Stopa, I. Roterman, L. Konieczny, Congo red-stabilized intermediates in the lambda light chain transition from native to molten state, Biochimie 78 (1996) 183–189.
[64] D.C. Carter, J.X. Ho, Structure of serum albumin, Adv. Protein Chem. 45 (1994) 153–203.